

1 **A transcriptional complex of FtMYB102 and FtbHLH4 coordinately regulates the accumulation of**
2 **rutin in *Fagopyrum tataricum***

3 **Running title: Transcriptional complex FtMYB102 and FtbHLH4 regulates rutin accumulation**

4 Yaolei Mi^{1,3*}, Yu Li^{3,4*}, Guangtao Qian³, Lucas Vanhaelewyn^{5,6}, Xiangxiao Meng³, Tingxia Liu³, Wei
5 Yang³, Yuhua Shi³, Pengda Ma⁷, Atia-tul-Wahab⁸, Shilin Chen^{3#}, Wei Sun^{3#}, Dong Zhang^{1,2#}

6
7 ¹College of Agriculture, South China Agricultural University, Guangzhou 510642, China

8 ²Guangdong Laboratory for Lingnan Modern Agriculture, Guangzhou 510642, China

9 ³Key Laboratory of Beijing for Identification and Safety Evaluation of Chinese Medicine, Institute of
10 Chinese Materia Medica, China Academy of Chinese Medical Sciences, Beijing 100700, China

11 ⁴Industrial Crop Research Institute, Sichuan Academy of Agricultural Sciences, Chengdu 610300, China

12 ⁵Deroose Plants NV., Weststraat 129 A, 9940 Sleidinge, Belgium

13 ⁶Department of Agricultural Economics, Ghent University, Coupure Links 653, B-9000 Ghent, Belgium

14 ⁷Northwest A&F University, Yangling 712100, China

15 ⁸Center for Molecular Medicine and Drug Research, International Center for Chemical and Biological
16 Sciences, University of Karachi, Karachi 75270, Pakistan

17 *These authors contributed equally to this work.

18 #Address correspondence to slchen@icmm.ac.cn, wsun@icmm.ac.cn or dzhang@scau.edu.cn

19 **Abstract**

20 Tartary buckwheat is rich in flavonoids, which not only play an important role in plant-environment
21 interaction, but are also beneficial to human health. Rutin is a therapeutic flavonol which is massively
22 accumulated in Tartary buckwheat. It has been demonstrated that transcription factors control rutin
23 biosynthesis. However, the transcriptional regulatory network of rutin is not fully clear. In this study,
24 through transcriptome and target metabolomics, we validated the role of FtMYB102 and FtbHLH4 TFs at
25 the different developmental stages of Tartary buckwheat. The elevated accumulation of rutin in the sprout
26 appears to be closely associated with the expression of FtMYB102 and FtHLH4. Yeast two-hybrid,

27 transient luciferase activity and co-immunoprecipitation demonstrated that FtMYB102 and FtbHLH4 can
28 interact and form a transcriptional complex. Moreover, yeast one-hybrid showed that both FtMYB102 and
29 FtbHLH4 directly bind to the promoter of chalcone isomerase (*CHI*), and they can coordinately induce *CHI*
30 expression as shown by transient luciferase activity assay. Finally, we transferred the FtMYB102 and
31 FtbHLH4 into the hairy roots of Tartary buckwheat and found that they both can promote the accumulation
32 of rutin. Our results indicate that FtMYB102 and FtbHLH4 can form a transcriptional complex by inducing
33 *CHI* expression to coordinately promote the accumulation of rutin.

34

35 **Keywords:** Tartary buckwheat (*Fagopyrum tataricum*), secondary metabolism, rutin, transcription factors,
36 transcriptional regulation, medicinal plants

37

38 INTRODUCTION

39 Flavonoids are major constituents of polyphenol in plant secondary metabolites. They consist mainly of
40 anthocyanins, proanthocyanidins (PAs), flavonols, and flavones, which are present in almost all higher
41 plants

42 (Williams and Grayer, 2001). Flavonoids play critical roles in plant–environment interactions, including
43 those involved in being uvioresistant, anti-herbivore and anti-pathogen (Emiliani *et al.* 2013; Barbehenn *et*
44 *al.* 2011). Additionally, they also contribute to human nutrition and health (Williams *et al.* 2004). Rutin
45 (quercetin-3-O-rutinoside), known as vitamin P, is a therapeutic flavonol bearing cytoprotective effects
46 (Negahdari *et al.* 2021), which is massively accumulated in the seeds and leaves of Tartary buckwheat
47 (Jiang *et al.* 2007). Previous studies have primarily focused on seeds, with few investigations on seedlings.

48 The gene encoding flavonoid biosynthetic enzymes for the major flavonoid skeleton has been identified
49 decades ago. Briefly, the pathway begins with phenylalanine and forms an important intermediate product,
50 naringenin chalcone. Several key enzymes catalyze this precursor, such as phenylalanine aminolyase (PAL),
51 cinnamic acid-4-hydroxylase (C4H), 4-coumarate-CoA ligase (4CL), and chalcone synthase (CHS)
52 (Russell, 1971; Dixon & Lamb, 1979; Koes *et al.* 1989). Then, chalcone isomerase (CHI) catalyzes the
53 resulting naringenin chalcone to form naringenin (Mona & Christopher, 1987). Furthermore, naringenin
54 can be converted to flavones under the action of flavone synthase (FNS). Flavanone 3-hydroxylase (F3H),
55 flavanone 3'-hydroxylase (F3'H), and flavonoid 3'5'-hydroxylase (F3'5'H) are responsible for producing
56 dihydroflavonols which are precursors to flavonol and anthocyanidin branch (Hagmann *et al.* 1983; Cheng
57 *et al.* 2014). The dihydroflavonols are subsequently catalyzed by flavonol synthase (FLS) to produce
58 flavonols (Holton *et al.* 1993), among which rutin is a trademarked compound of Tartary buckwheat.
59 *FtUGT73BE5* was characterized to be involved in rutin's subsequent glycosylation (Yin *et al.*, 2020).

60 Additionally, the enzyme dihydroflavonol reductase (DFR), which is following anthocyanidin synthase
61 (ANS) and anthocyanidin reductase (ANR), contribute to converting dihydroquercetin to proanthocyanidin
62 (e.g., epicatechin) (Liew *et al.* 1998). Another pathway is the conversion of dihydroquercetin to catechin
63 catalyzed by DFR and leucoanthocyanidin reductase (LAR).

64 Transcription factors (TFs) are the key factors to realize the spatiotemporal regulation patterns of secondary
65 metabolites (Yang *et al.* 2012). Many TFs that regulate flavonoids synthesis have been reported, of which
66 MYB is a crucial factor (Du *et al.* 2010; Vimolmangkang *et al.* 2013; Zhou and Memelink, 2016; Luo *et al.*
67 2018). MYB is one of the largest members of the plant transcription factor families and is classified into
68 four types according to the number of MYB domain repeats (represented by R). The classes comprise of
69 one MYB domain (R1/ R2-MYB), two (R2R3-MYB), three (R1R2R3-MYB), and four MYB domains
70 (4R-MYB), among which R2R3 MYB is essential for flavonoids regulation (Dubos *et al.* 2010). Several
71 MYB genes involved in flavonoids synthesis were first identified in *Arabidopsis thaliana*. For example,
72 *PAP1/AtMYB75*, *AtMYB90*, *AtMYB113*, and *AtMYB114* in *Arabidopsis* from MYBA/SG6 play a positive
73 regulatory role for anthocyanin accumulation by regulating *UFGT* and *DFR* expression (Zimmermann *et al.*
74 2004; Teng *et al.* 2005; Gonzalez *et al.* 2008; Lotkowska *et al.* 2015). The flavonol branch of the flavonoid
75 biosynthesis is controlled in *Arabidopsis* by *MYB11*, *MYB12*, and *MYB111* from subgroup 7 of the
76 R2R3-MYB family, which activates *CHS*, *CHI*, *F3H*, and *FLS*. However, *MYB3*, *MYB4*, *MYB7*, and
77 *MYB32* with C2 repressors belonging to SG4 play an inhibitory role in the flavonoid synthesis pathway (Jin
78 *et al.* 2000; Teng *et al.* 2005; Gonzalez *et al.* 2008; Zhou *et al.* 2015, 2017). In Tartary buckwheat, several
79 MYBs have been reported to be involved in regulating the synthesis of flavonoids. Bai *et al.* (2014)
80 reported that the overexpression of *FtMYB1* and *FtMYB2* significantly enhanced the accumulation of
81 proanthocyanidins in *Nicotiana benthamiana* (*N. benthamiana*). *FtMYB31* is highly expressed in seeds and

82 has been reported to positively regulate the biosynthesis of rutin in *N. benthamiana* (Hou *et al.*, 2021).
83 Likewise, FtMYB11, and FtMYB13-16 act as negative regulators of rutin biosynthesis (Zhou *et al.* 2017;
84 Zhang *et al.* 2018). Zhang *et al.* (2019) reported that light-induced *FtMYB116* can promote the
85 accumulation of rutin. SG4-like *FtMYB18* and *FtMYB8* with tissue-specific expression patterns were
86 recently identified as repressors of accumulating anthocyanin and proanthocyanidin (Huang *et al.*, 2019;
87 Dong *et al.*, 2020). However, the fine molecular mechanism of MYB's regulation of flavonoids synthesis in
88 Tartary buckwheat is still not well understood.

89 Generally, MYB recruits basic helix-loop-helix (bHLH) and WD40 proteins to form canonical
90 MYB-bHLH-WDR (MBW) regulatory complexes to control flavonoid synthesis *in planta*. Several bHLHs
91 modulating the anthocyanin and proanthocyanidin synthesis have been identified in dicots, including *AN1*
92 and *JAF14* in *Petunia* (Spelt *et al.* 2000; Montefiori *et al.* 2015), *Delila* and *Mutabilis* in snapdragon (Shang
93 *et al.* 2011), *TT8* and *GLABRA3* in *Arabidopsis* (Nesi *et al.* 2000; Payne *et al.* 2000), *MtTT8* in *Medicago*
94 *truncatula* (Li *et al.* 2016). The pleiotropic bHLHs regulate the binding affinity of MYB to the *cis*-element
95 of the target gene (Hichri *et al.*, 2011) via interaction with the R3 repeat domain in R2R3 MYB proteins
96 (Grotewold *et al.*, 2000). Interestingly, MYB regulating flavonol synthesis requires bHLH in maize (Goff *et*
97 *al.*, 1992), however, in *Arabidopsis* and grapevine it is independent of bHLH (Czemmel *et al.* 2009).
98 However, relatively few bHLHs have been reported in Tartary buckwheat, with only FtTT8 reported to
99 interact with other MYB TFs to regulate anthocyanin/proanthocyanidin synthesis (Huang *et al.* 2019; Dong
100 *et al.* 2020; Wang *et al.* 2022). To date, the mechanism of bHLH regulation of flavonoids, as well as how
101 MYB and bHLH synergistically regulate flavonoid synthesis remain largely elusive in Tartary buckwheat.
102 In this study, we identified and characterized two novel regulators, FtMYB102 and FtBHLH4, forming a
103 transcriptional complex that co-regulates flavonoid synthesis, particularly flavonol, from sprout to seedling

104 development. These results may have profound impacts on the understanding of precise transcriptional
105 regulatory mechanisms of flavonoid production and even other secondary metabolites.

106 **MATERIALS AND METHODS**

107 **Plant material and growth conditions**

108 Two Tartary buckwheat varieties, TB115 and TB128, were used in this study. The growth conditions of
109 Tartary buckwheat were previously reported (Zhang *et al.*, 2019). In brief, Tartary buckwheat seed coats
110 were peeled off by soaking seeds in water for 20 min. Peeled seeds were then sterilized by washing with 75%
111 ethanol for 1 min followed by 10 % sodium hypochlorite for 8 min and six 1-min washes with sterilized
112 water. Next, the seeds were inoculated into sterile medium (Murashige and Skoog (MS) medium containing
113 0.8% agar and 1% sucrose). Subsequently, the sprouts and seedlings were harvested 3 and 8 days after
114 sowing while kept at a photoperiod of 16h (light)–8h (dark) ($\sim 150\mu\text{molm}^{-2}\text{ s}^{-1}$) at 25°C, respectively. The
115 plant samples were frozen immediately using liquid nitrogen and stored at –80°C for further use.

116 **RNA sequencing**

117 The total RNA of Tartary buckwheat was extracted according to the manufacturer’s instructions (Tiangen,
118 Beijing, China). RNA quality was then evaluated and the integrity number (RIN) of the samples was >8.0
119 using a Bioanalyzer 2100 instrument (Agilent Technologies, Palo Alto, CA, US). RNA sequencing was next
120 conducted after establishing sequencing libraries using an IlluminaXten sequencing system (Illumina Inc.,
121 San Diego, CA, USA) as per the manufacturer’s instructions.

122 **RNA-seq data and phylogenetic analysis**

123 After removing the low-quality bases and Illumina adapter sequences, approximately 46.9 G bases of clean
124 data were utilized for this analysis. The STAR v.2.5 software was used to map these reads to the published
125 Tartary buckwheat reference genome (Zhang *et al.* 2017a). Based on their FPKM (reads per kilobase of

126 exon per million mapped reads) values (Mortazavi *et al.* 2008) differentially expressed genes (DEGs) were
127 then sifted. FPKM values and DEG analysis (\log_2 Fold change ≥ 1) were analyzed using Htseq and
128 DESeq2 software, respectively. The alignment of amino acid sequences with the default parameters and
129 construction of phylogenetic tree was performed by using the neighbor-joining method via MEGA V.6
130 (Kumar *et al.* 2016). Bootstrap analyses with 1000 replications were used to assess the phylogenetic tree's
131 reliability nodes.

132 **Coexpression analysis**

133 TFs were identified by using hmmscan software. Four genes, *C4H* (FtPinG0001575100), *F3H*
134 (FtPinG0006662600), *F3'H* (FtPinG0002353900), and *CHI* (FtPinG0002790600), were used in
135 coexpression analysis with a default value 0.05 to screen TFs that participated in the regulation of rutin
136 synthesis. The paired genes were considered significantly coexpressed if the Pearson correlation coefficient
137 (r) was greater than 0.95 (Ariani & Gepts, 2015).

138 **Quantitative RT-PCR**

139 After the total RNA of Tartary buckwheat was isolated, the first-strand cDNA was synthesized using a
140 commercial kit (TransGen, Beijing, CN) and then diluted to a concentration at 1 $\mu\text{g}/\text{ml}$ for qRT-PCR using
141 TransStart[®] Green qPCR SuperMix UDG (TransGen, Beijing, China) according to the manufacturer's
142 instruction. Additionally, qRT-PCR was conducted at Rotor-Gene Q (Qiagen, Hilden, Germany) . The
143 experiment was conducted in triplicates, and the data were normalized to that of the reference gene, actin.
144 The primers for qRT-PCR are listed in Table S1.

145 **Gene amplification and vector construction**

146 Using high fidelity DNA polymerase and cDNA as the template, transcriptional factors were amplified.
147 Target gene promoters were amplified using the genome DNA of Tartary buckwheat as the template. The

148 primers are listed in Table S1. These genes were constructed in a Blunt-Zero cloning vector (TransGen,
149 Beijing, China) for further use.

150 **Yeast two-hybrid**

151 The pLexA-FtbHLH4 reporter was cotransformed with the p8op-LacZ plasmid into the yeast strain EGY48,
152 and positive clones were screened using the SD/-His/-Ura dropout media. After these clones were verified
153 to be nonself-activated and non-toxic to yeast, they were mixed with the yeast strain, YM4271 transformed
154 pB42AD-FtMYB102. Positive clones were obtained using SD/-His/-Ura/-Trp media with the addition of
155 20-mg/mL X-gal (5-Bromo-4-chloro-3-indolyl- β -D-galactopyranoside) for color development.

156 **Yeast one-hybrid**

157 The AD-FtMYB102 effector and AD-FtbHLH4 were cotransformed with the *CHI*p: *LacZ* reporter into the
158 yeast strain EGY48. After the transformants were screened for SD/-Trp-Ura dropout media, they were
159 further inoculated on the dropout media containing X-gal for color variation.

160 **Co-immunoprecipitation**

161 Briefly, bHLH4 and Myb102 fusions were transiently expressed in 5-week-old leaves of *Nicotiana*
162 *benthamiana*, and infiltrated leaves were harvested 72 h after inoculation. Two grams of the corresponding
163 leaves were ground in liquid nitrogen and inoculated in lysis buffer (50-mM Tris-MES, pH 8.0, 500-mM
164 sucrose, 1-mM MgCl₂, 10-mM EDTA, 5-mM dithiothreitol, 1-mM PMSF, and 1-mM Cocktail protease
165 inhibitors) with end over end shaking for 30 min on ice. After centrifugation at 15,000 g for 1 h at 4°C, the
166 supernatant was filtered and collected using MiraCloth. The protein concentrations of
167 co-immunoprecipitation mixtures were then diluted to 1-mg/mL. Next, 500 μ L of the above samples were
168 precleared by incubating with protein G agarose beads at 4°C. After centrifugation, the precleared
169 supernatant was incubated with protein G agarose beads conjugated rabbit-anti-GFP antibody (Yeason, CN)

170 overnight at 4°C. Subsequently, the beads were collected by five times centrifugation-wash and eluted with
171 50-μL glycine aqueous solution (pH 2.5) for 1 min, and then 5-μL Tris pH 9.0 was added to neutralize. The
172 eluted fractions and crude extracts were run in 10% SDS-PAGE gel and subjected to immunoblots with the
173 corresponding antibodies. For the immunoblots, the primary monoclonal antibodies mouse-anti-Myc and
174 mouse-anti-GFP (TransGen Biotech, CN) were used followed by secondary antibodies
175 Goat-anti-Mouse-IgG horseradish peroxidase. An enhanced chemiluminescent reagent (StarLighter, CN)
176 was used to detect the signal.

177 **Dual-luciferase reporter assay**

178 The *35S-Ren-CHIp:LUC* reporter plasmid, construct *pGreen-62SK-FtMYB102*, and
179 *pGreen-62SK-FtbHLH4* effector mixture were transformed into *Agrobacterium tumefaciens* strain EHA105,
180 which were subsequently injected into the leaves of 5-week-old *N. benthamiana*. The tobacco leaves were
181 harvested after growing under dark conditions overnight and subsequently under a 14 h light /10 h dark
182 photoperiod for 4 days. The samples were handled as per instruction of the Dual-luciferase® Reporter
183 Assay System (E1920, Promega, USA), and the signal was detected using SpectraMax i3x (Molecular
184 Devices, USA).

185 **Luciferase complementation assay**

186 The FtMYB102 and FtbHLH4 were constructed into plasmids of pCAMBIA1300-NLuc and
187 pCAMBIA1300-CLuc, respectively. Both fusion proteins were then expressed in *N. benthamiana* by
188 *Agrobacterium*-mediated transient expression. After the plants were placed in the dark for 1 day and
189 photoperiod for 48 h, luciferase substrate and beetle luciferin (E1602, Promega, USA) at 150-μg/ml in
190 saline were evenly sprayed on the back of *N. benthamiana* leaves. Luminescence was observed using
191 NightSHADE LB985 (Berthold, Germany) after placing these leaves in the dark for 7 min.

192 **Transformation of the hairy roots of Tartary buckwheat**

193 When the two pieces of cotyledon of Tartary buckwheat seedlings were unfolded, the hypocotyls and
194 cotyledons, which were cut into ~0.5-cm segments and sheared into 0.5-cm pieces, respectively, were
195 selected as explants. Then, these explants were infected with *Agrobacterium rhizogenes* ACC10060 strain
196 transformed target gene plasmids for 10 min after preculturing them on an MS solid medium for 1 day.
197 Next, the explants were placed on an MS solid medium containing 500-mg/ml cefotaxime under 14 h
198 light/10 h dark photoperiod at 25°C after coculturing them with bacteria for 3 days in the dark. The hairy
199 roots were cut into 2–3 cm pieces and propagated in liquid MS medium (containing 30 g/L sucrose) at 25°C
200 with a rotation speed of 80 rpm when they occurred and grew approximately 1–2 weeks later.

201 **Sample treatment and LC–MS analysis**

202 Samples stored at –80°C were ground into fine powder. Then, 0.1 g of each sample was extracted in
203 1.0-mL 70% methanol aqueous at 4°C overnight and ultrasonicated for 30 mins. After centrifugation, 0.2
204 mL of each supernatant was filtered via a 0.22 µm membrane for liquid chromatography–mass
205 spectrometry (LC–MS) analysis. The chromatographic conditions used for LC–MS were as the
206 previous investigation (Yang, et al, 2020).

207 **RESULTS**

208 **Flavonoid content varies in sprouts and seedlings**

209 The secondary metabolites of plants have spatiotemporal characteristics, which means that the
210 accumulation of secondary metabolites varies in different tissues and at different developmental stages. In
211 addition to its seeds, Tartary buckwheat sprouts are also of great value. Therefore, we focused on the
212 dynamic change in flavonoid content in Tartary buckwheat after germination. The sprouts and seedlings
213 were harvested after sowing for 3 and 8 d, respectively. As shown in Figure 1A, the etiolated sprouts just

214 emerged with their cotyledons still closed, yellow, and an apical hook. After 8 days, the cotyledons were
215 fully open and green and the hypocotyls were fully grown. Target metabolomics showed more flavonoids,
216 such as kaempferol, quercitrin, rutin, catechin, and epicatechin existed in the sprouts compared with the
217 seedlings from two representative varieties TB115 and TB128 (Figure 1B & Table S2).

218

219 **Comparative analysis of transcriptional profiles**

220 RNA sequencing was performed using the two varieties (TB115 and TB128) at the sprout and seedling
221 stage to reveal the molecular mechanism that accounts for the differences in flavonoid contents of Tartary
222 buckwheat at different developmental stages (accession number: PRJNA762576). We calculated the
223 upregulated and downregulated genes of sprouts compared with seedlings. There were 3,215 and 3,084
224 genes upregulated in TB115 and TB128, respectively, with a total of 2,152 genes upregulated in both
225 varieties (Figure 2A). The number of genes downregulated in TB115 and TB128 were 3,059 and 2,876,
226 respectively, of which 1,855 genes were in common (Figure 2B). Following that, because flavonoid content
227 was higher in sprouts than in seedlings, GO analysis was performed on the 2,152 upregulated genes (Figure
228 2C). The majority of the genes were discovered to be related to cell growth, which is consistent with the
229 expectation that the seedlings were in the rapid growth stage. Interestingly, we discovered that the
230 phenylpropanoid and secondary metabolic pathways both had a substantial number of annotated genes,
231 which confirmed our previous metabolome results, indicating that a large number of secondary metabolites
232 change in plants during these two stages.

233

234 **Expression of genes related to flavonoid biosynthesis**

235 We specifically analyzed the expression of genes related to flavonoid synthesis. The results showed that the

236 expression of most of these genes in sprouts was higher in sprouts than in seedlings (Figure 3 & Table S3).
237 For example, two out of the five transcripts of *PAL* (FtPinG0001546000 and FtPinG0005713400), three
238 *CHS* (FtPinG0000551600, FtPinG0000551900, and FtPinG0008806400) and two *4CL* (FtPinG0003957300
239 and FtPinG0005072700) displayed a much higher expression level in the sprouts compared to seedlings.
240 Additionally, *C4H* (FtPinG0001575100), *F3'H* (FtPinG0002353900), *F3H* (FtPinG0006662600 and
241 FtPinG0008251700), *DFR* (FtPinG0002371500), *FLS* (FtPinG0006907100), *CHI* (FtPinG0002790600),
242 and *GTR* (FtPinG0006606900) displayed a similar pattern. The expression patterns of these flavonoid
243 structure genes were consistent with the flavonoid content described previously (Figure 1B), indicating that
244 sprouts accumulate more flavonoids than seedlings. After that, we performed real-time quantitative
245 RT-PCR for further validation of the expression of flavonoid structure genes. The results showed that the
246 expression levels of these genes in the sprouts were significantly higher than those in seedlings (Figure S1),
247 which was also consistent with our transcriptome results.

248

249 **Coexpression revealed that FtMYB102 directly regulated *CHI* expression**

250 To obtain the potential TFs involved in flavonoid biosynthesis, coexpression was performed to identify the
251 TFs, which are tightly coexpressed with four highly expressed structural genes: *C4H* (FtPinG0001575100),
252 *F3H* (FtPinG0006662600), *F3'H* (FtPinG0002353900), and *CHI* (FtPinG0002790600). We identified 19,
253 29, 29, and 41 TFs that were coexpressed among *C4H*, *CHI*, *F3H*, and *F3'H*, respectively, through this
254 analysis (Table S4 and S5). Among these TFs, 14 were tightly coexpressed with all the four genes (Figure
255 4A). Similarly, all these 14 TFs exhibited higher expression in sprouts than in seedlings in a pattern similar
256 to *C4H*, *CHI*, *F3H*, and *F3'H* (Figure 4B), where the largest gene family (4 MYBs out of 14 TFs) were
257 proposed to directly regulate the synthesis of flavonoids.

258 MYB TFs that regulated flavonoid synthesis were also identified using the yeast one-hybrid assay (Y1H).
259 The promoters of *C4H*, *CHI*, *F3H*, and *F3'H* were cloned into pLacZ-2 μ reporter vectors in fragments
260 (2,000 bp), while the four MYB TFs were cloned into pB42AD (GAL4 activation domain [AD] fused).
261 FtPinG0007148200.01, which we termed FtMYB102, is bound to the promoter of *CHI*, but not to the
262 promoters of the other three examined genes, as shown in Figure 5A (data not shown). Sprouts accumulated
263 more *FtMYB102* transcripts than seedlings (Figure 5B). Further analysis showed FtMYB102 coded for 265
264 amino acids and the phylogenetic relationship revealed that FtMYB102 clustered with AtMYB5 (Figure 6A
265 & Figure S2A), regulating the accumulation of PA (Deluc *et al.* 2008) together with PhPH4(*Petunia*
266 *hybrida*), MdMYB12(*Malus domestica*), and VvMYB5b(*Vitis vinifera*), which belonged to classic R2R3
267 MYB TFs (Figure 6B).

268

269 **bHLH candidate genes involved in flavonoid synthesis**

270 Generally, bHLH TFs are able to interact with MYB TFs to form a transcription complex that regulates the
271 expression of flavonoid synthesis genes. It was previously reported in *Arabidopsis thaliana* that TT8 can
272 form a complex with the MYB transcription factor to regulate the synthesis of flavonoids (Zhou *et al.*
273 2012). In this study, we identified seven homologous genes named *FtbHLH1–FtbHLH7* in Tartary
274 buckwheat based on the TT8 sequence alignment in *A. thaliana*. Then, we performed a phylogenetic
275 analysis of these seven genes to construct an evolutionary tree with other *Arabidopsis* bHLH TFs (Figure
276 S2B). Among them, FtbHLH1 and FtbHLH3–4 were classified as IIIf, while FtbHLH2 and FtbHLH5–7
277 were classified as III(d+e). Interestingly, many bHLH genes reported in *A. thaliana* and rice that were
278 involved in flavonoid synthesis belonged to the IIIf subfamily, (Ludwig *et al.* 1989; Feyissa *et al.* 2009;
279 Zhou *et al.* 2012), which indicated that FtbHLH1, FtbHLH3-4 were involved in the synthesis of flavonoids.

280 To further verify whether the three bHLH TFs participated in the regulation of flavonoids, Y1H was used to
281 clarify whether they can directly bind to the promoters of the flavonoid synthesis genes. As described above,
282 fragments (2,000 bp) of the promoters of *C4H*, *CHI*, *F3H*, and *F3'H* were cloned into pLacZ-2 μ reporter
283 vectors, whereas the three bHLH TFs were cloned into pB42AD. FtbHLH4 bound to the *CHI* promoter but
284 not to the other three promoters as shown in Figure 5A, whereas FtbHLH1 and FtbHLH3 could not bind to
285 any promoters (data not shown). As a result, we focused our research on FtbHLH4. Similar to FtMYB102,
286 we found that the expression of FtbHLH4 was significantly higher in sprouts than in seedlings (Figure 5C).
287 As shown, the expression patterns of FtMYB102 and FtbHLH4 genes were found to be consistent with
288 those of flavonoid synthesis genes, suggesting that the two genes directly regulated the expression of
289 flavonoid synthesis genes.

290

291 **FtbHLH4 physically interacts with FtMYB102**

292 To identify whether MYB102 and bHLH4 can form a complex, yeast two-hybrid experiment (Y2H) was
293 performed by fusing FtbHLH4 with the LexA DNA-binding domain and the FtMYB102 with the B42
294 activation domain (AD), respectively. Y2H results showed that LacZ reporter expression was strongly
295 induced when both FtbHLH4 and FtMYB102 were simultaneously transformed into yeast, but either
296 individual or none was effective, indicating FtbHLH4 could interact with FtMYB102 in yeast (Figure 7A).
297 Next, a transient luciferase activity assay was performed in *N. benthamiana* to further examine the
298 interaction between FtbHLH4 and FtMYB102. As shown in Figure 7B, no or weak luciferase fluorescence
299 signal was observed in leaves of *N. benthamiana* injected with water, nLUC+cLUC, nLUC+
300 FtbHLH4-cLUC, and FtMYB102-nLUC+cLUC. However, when leaves were injected with
301 FtMYB102-nLUC+ FtbHLH4-cLUC, there was a significant increase in the fluorescence value of leaves.

302 The signal of FtMYB102-nLUC+ FtbHLH4-cLUC increased more than 400 times when compared to the
303 control groups (Figure 7C). Furthermore, we conducted co-immunoprecipitation assays to verify the
304 FtbHLH4–FtMYB102 interaction. To achieve this assay, 35S:FtMYB102-MYC was coinfiltrated with
305 35S:GFP and 35S:FtbHLH4-GFP inserted into *N. benthamiana* leaves. Afterward, the total plant proteins
306 were extracted. Immunoprecipitation was conducted with the GFP antibody linked to agarose beads, where
307 the FtMYB102-MYC fusion protein was pulled down in samples coexpressing FtbHLH4-GFP, but not GFP
308 alone (Figure 7D). Therefore, these results indicate that FtbHLH4 interacted with FtMYB102.

309

310 **FtMYB102 and FtbHLH4 Coordinate Activation the Expression of *CHI***

311 Previous studies have suggested that MYB and bHLH formed complexes that regulated the expression of
312 flavonoids synthesis genes. To study the regulation pattern of downstream gene expression by FtMYB102
313 and FtbHLH4, a dual-luciferase reporter assay was performed in *N. benthamiana* (Figure 8A). Figure 8B
314 showed that there was no LUC signal difference between 62SK (*Agrobacterium tumefaciens* strain GV3101
315 harboring recombinant plasmids), FtMYB102-62SK, FtbHLH4-62SK, and FtMYB102-62SK+
316 FtbHLH4-62SK co-transformed with empty *pGreenII 0800-LUC* vector into leaves, respectively. However,
317 when co-transformed with *ProFiCHI:LUC*, the LUC signal in the individual transformation with
318 FtMYB102-62SK and FtbHLH4-62SK was increased significantly than the 62SK control. In addition, the
319 LUC signal in the co-transformation of FtMYB102-62SK and FtbHLH4-62SK was further increased.
320 Therefore, the results indicated that FtbHLH4 and FtMYB102 can individually and coordinately activate
321 *CHI* expression via a complex.

322

323 **Overexpression of both FtMYB102 and FtbHLH4 can promote flavonoids biosynthesis**

324 To verify whether FtMYB102 and FtbHLH4 promoted the synthesis of flavonoids, we generated transgenic
325 Tartary buckwheat hair roots that overexpressed *FtMYB102* (OE-FtMYB102) and *FtbHLH4*
326 (OE-FtbHLH4). Three independent transgenic hairy root lines were used for further functional analysis.
327 The expression of *FtMYB102* or *FtbHLH4* in the three lines was significantly higher than that in the WT,
328 showing that both the genes were overexpressed in the transgenic hair roots according to qRT-PCR results
329 (Figure S3). Concomitantly, LC-MS analysis showed OE-FtMYB102 and OE-FtbHLH4 produced more
330 flavonoids than WT (except catechin in MYB102OX-4 and MYB102-OX-6) (Figure 9A). The
331 overexpressing lines displayed a significant increase in rutin, indicating that FtMYB102 and FtbHLH4 had
332 greatly promoted rutin synthesis. The qRT-PCR analysis consistently revealed enhanced expressions of
333 *CHS*, *CHI*, *F3H*, and *FLS* in OE-FtMYB102 and OE-FtbHLH4 lines compared with the control (Figure
334 9B), suggesting that FtMYB102 and FtbHLH4 promote flavonoid synthesis through these four genes.

335 **DISCUSSION**

336 Tartary buckwheat is rich in flavonoids, especially its trademark rutin, and has a high nutritional and
337 medicinal value. This study showed that in addition to Tartary buckwheat seeds which are commonly
338 consumed (Yang *et al.* 2020), the flavonoid content of its sprouts and seedlings is considerably high. Given
339 that this vegetable has been gaining popularity in China, understanding its edible and medicinal value is
340 important. Secondary metabolite biosynthesis in plants is not only tissue-specific but also dependent on the
341 plant's developmental stages. According to Czechowski *et al.* (2016), the content of artemisinin increased
342 gradually during the development of a young leaf to its mature form. Arce-Rodríguez *et al.* (2017) showed
343 that capsaicinoid accumulation is dependent on the developmental stage of chili pepper fruits. As a result,
344 two Tartary buckwheat varieties were used in this study to investigate the flavonoid content during two
345 developmental stages (sprouts and seedlings). The results of the metabolome showed that the content of

346 most flavonoids was higher in the sprouts than in the seedlings. Most previous studies on the flavonoid
347 content of Tartary buckwheat have focused on seeds. As a result, this study is critical in determining the
348 flavonoid content of Tartary buckwheat in the different developmental stages. Follow-up consumption
349 studies might be an interesting research topic.

350 To reveal the transcriptional mechanism of flavonoid accumulation at the sprout and seedling stages, RNA
351 sequencing and coexpression analysis was performed. TFs coexpressed with four flavonoid synthetic genes
352 (*CHI*, *F3H*, *F3' H*, and *C4H*) were screened. The observations showed that one of the MYB TFs, namely
353 FtMYB102, showed a consistent expression pattern with all the four genes. Y1H showed that FtMYB102
354 directly binds to the promoter of *CHI*. Then, a transient luciferase activity assay was conducted in *N.*
355 *benthamiana* to demonstrate that FtMYB102 promoted *CHI* expression (Figure 8B). A new MYB
356 transcription factor was discovered here that regulated flavonoid synthesis at different Tartary buckwheat
357 development stages. FtMYB102 clustered with AtMYB5, which does not belong to the SG7 group of
358 MYBs that particularly control flavonol accumulation, in an unusual phylogenetic relationship (Wang *et al.*
359 2017). AtMYB5 and its homology in grape, VvMYB5b, have generally been considered a regulator of PA
360 (Deluc *et al.* 2008). The overexpression of FtMYB102 not only significantly promoted PA accumulation
361 but also flavonol accumulation in this study (Figure 9A), which further broaden the roles of MYB5 genes
362 on flavonoid synthesis regulation.

363 Generally, bHLH proteins act as transcriptional factors, subtly controlling flavonol metabolism via the
364 affinity of *cis*-regulatory element of downstream genes (Li *et al.* 2020), broad or restricted expression
365 pattern, influenced by their dimerization properties with MYB TFs (Feller *et al.* 2011). They directly bind
366 to the *cis*-elements (G-box and E-box) of structural genes via the basic region, located at the N-terminal
367 end of the domain, while the HLH region, at the C-terminal end, is involved in homo- and

368 hetero-dimerization (Toledo-Ortiz et al. 2003). In this study, we detected seven homologs of AtTT8 in the
369 Tartary buckwheat genome, which exert distinct DNA-binding functions, i.e., only FtbHLH4 binds to *CHI*
370 promoter but others are not able to, which could explain the specific binding of bHLH members to
371 *cis*-elements to regulate flavonoid synthesis. FtbHLH4 was found to be more highly expressed in sprouts
372 than in seedlings, and it resembled FtMYB102, suggesting that FtbHLH4 regulates sprout and seedling
373 flavonoid biosynthesis. The regulation of flavonoids in Tartary buckwheat was also confirmed by the
374 overexpression of *FtbHLH4* in hairy roots, which leads to the accumulation of flavonoids.

375 It has also been reported that MYB TFs can interact with bHLH to form a complex that regulates gene
376 expression in *Arabidopsis thaliana* (Gonzalez et al. 2008); however, this has not been reported in Tartary
377 buckwheat. In this study, Y2H, transient luciferase activity assay, and CoIP demonstrated that FtbHLH4 can
378 interact with the FtMYB102 (Figure 7). Furthermore, through transient luciferase activity assay, it was
379 shown that when both MYB102 and bHLH4 TFs were present, the activation of *CHI* was significantly
380 stronger than when they were present independent of each other (Figure 8). These results indicate that
381 MYB102 and bHLH4 interacted with each other to form a complex that directly bound to the *CHI* promoter
382 and actively triggered *CHI* gene expression. Our results strongly suggest that the combined action of
383 FtMYB102 and FtHLH4, which enhances target gene *CHI* expression, is critical for high flavonoid
384 production (Figures 1, 7–9). These findings highlight the importance of the interaction specificity between
385 the cooperative partners of FtMYB102 and FtHLH4 proteins in regulating flavonoid metabolism at the
386 sprout and seedling stages.

387 Based on the results, we developed a working model (Figure 10). In the sprout stage, the highly expressed
388 MYB102 and bHLH4 interact to form a transcriptional complex that directly binds to the promoter of *CHI*
389 and induces its expression. *CHI* is an essential catalytic enzyme in the rutin synthesis pathway. Under its

390 catalysis, naringenin chalcone is transformed into chalcone, and rutin is further synthesized under the
391 action of several other catalytic enzymes. Therefore, when the expression level of *CHI* is high, the
392 synthesis of rutin is increased, resulting in the formation of high rutin in sprouts. In the seedling stage, the
393 expression of MYB102 and bHLH4 decreased, resulting in decreased *CHI* expression, ultimately reducing
394 the content of rutin in the seedlings. It remains unknown what factors cause the difference in the
395 transcription levels of MYB102 and bHLH4 when Tartary buckwheat is in different developmental stages.
396 Since many differences are observed when plants are at different stages of development, the changes in the
397 expression of these two TFs could have been produced by a hormone or a single signal molecule. Hence,
398 further research is needed to address this issue.

399

400 **Acknowledgments**

401 This work was supported by the following grants and projects: National Key R&D Program of China
402 (2019YFC1711100, 2021YFE1011900), Scientific and Technological Innovation Project of China
403 Academy of Chinese Medical Sciences (CI2021A03710, CI2021A041013), Opening project of Shanghai
404 Key Laboratory of Plant Functional Genomics and Resources, National Natural Science Foundation of
405 China (31860408, 31900258).

406

407 **Conflict of interests**

408 The authors declare that there is no conflict of interests regarding the publication of this article.

409

410 **References**

411 Arce-Rodríguez M.L, Ochoa-Alejo N. 2017. An R2R3-MYB transcription factor regulates capsaicinoid
412 biosynthesis. *Plant Physiol*, 174, 1359-1370.

413 Ariani A, Gepts P. 2015. Genome - wide identification and characterization of aquaporin gene family in

- 414 common bean (*Phaseolus vulgaris* L.). *Mol Genet Genomics*, 290, 1771–1785.
- 415 Bai YC, Li CL, Zhang JW, Li SJ, Luo XP, Yao HP, Chen H, Zhao HX, Park SU, Wu Q. 2014.
- 416 Characterization of two Tartary buckwheat R2R3-MYB transcription factors and their regulation of
- 417 proanthocyanidin biosynthesis. *Physiol Plant*, 152, 431–40.
- 418 Barbehenn RV, Constabel CP. 2011. Tannins in plant–herbivore interactions. *Phytochemistry*, 72,
- 419 1551-1565.
- 420 Cheng AX, Han XJ, Wu YF, Lou HX. 2014. The function and catalysis of 2-oxoglutarate-dependent
- 421 oxygenases involved in plant flavonoid biosynthesis. *Int J Mol Sci*, **15**, 1080–1095.
- 422 Czechowski T, Larson TR, Catania TM, Harvey D, Brown GD, Graham IA. 2016. *Artemisia annua* mutant
- 423 impaired in artemisinin synthesis demonstrates importance of nonenzymatic conversion in terpenoid
- 424 metabolism. *Proc Natl Acad Sci U S A*, 113, 15150-15155.
- 425 Czemplin S, Stracke R, Weisshaar B, Cordon N, Harris NN, Walker AR, Robinson SP, Bogs J. 2009. The
- 426 grapevine R2R3-MYB transcription factor VvMYB1 regulates flavonol synthesis in developing grape
- 427 berries. *Plant Physiol*, **151**, 1513–1530.
- 428 Deluc L, Bogs J, Walker AR, Ferrier T, Decendit A, Merillon JM, Robinson SP, Barrieu F. 2008. The
- 429 transcription factor VvMYB5b contributes to the regulation of anthocyanin and proanthocyanidin
- 430 biosynthesis in developing grape berries. *Plant Physiol*, 147, 2041–2053.
- 431 Dixon RA, Lamb CJ. 1979. Stimulation of de novo synthesis of L-phenylalanine ammonia-lyase in relation
- 432 to phytoalexin accumulation in *Colletotrichum lindemuthianum* elicitor-treated cell suspension cultures
- 433 of French bean (*Phaseolus vulgaris*). *Biochim Biophys Acta*, **586**, 453–463.
- 434 Dong Q, Zhao H, Huang Y, Chen Y, Wan M, Zeng Z, Yao P, Li C, Wang X, Chen H, Wu Q. 2020.
- 435 FtMYB18 acts as a negative regulator of anthocyanin/proanthocyanidin biosynthesis in Tartary

- 436 buckwheat. *Plant Mol Biol*, 104, 309-325.
- 437 Du H, Huang Y, Tang Y. 2010. Genetic and metabolic engineering of isoflavonoid biosynthesis. *Appl*
438 *Microbiol Biotechnol*, **86**, 1293–1312.
- 439 Dubos C, Stracke R, Grotewold E, Weisshaar B, Martin C, Lepiniec L. 2010. MYB transcription factors in
440 Arabidopsis. *Trends Plant Sci*, 15, 573-581.
- 441 Emiliani J, Grotewold E, Ferreyra MLF, Casati P. 2013. Flavonols protect Arabidopsis plants against UV-B
442 deleterious effects. *Mol Plant*, 6, 1376-1379.
- 443 Feller A, Machemer K, Braun EL, Grotewold E. 2011. Evolutionary and comparative analysis of MYB and
444 bHLH plant transcription factors. *Plant J*, 66, 94-116.
- 445 Feyissa DN, Løvdaal T, Olsen KM, Slimestad R, Lillo C. 2009. The endogenous GL3, but not EGL3, gene is
446 necessary for anthocyanin accumulation as induced by nitrogen depletion in Arabidopsis rosette stage
447 leaves. *Planta* **230**, 747–754.
- 448 Goff SA, Cone KC, Chandler VL. 1992. Functional analysis of the transcriptional activator encoded by the
449 maize B gene: evidence for a direct functional interaction between two classes of regulatory proteins.
450 *Genes Dev*, 6, 864-875.
- 451 Gonzalez A, Zhao M, Leavitt JM, Lloyd AM. 2008. Regulation of the anthocyanin biosynthetic pathway by
452 the TTG1/bHLH/Myb transcriptional complex in Arabidopsis seedlings. *Plant J*, **53**, 814–827.
- 453 Hagemann ML, Heller W, Grisebach H. 1983. Induction and characterization of a microsomal flavonoid
454 3'-hydroxylase from parsley cell cultures. *Eur J Biochem*, **134**, 547–554.
- 455 Hao Y, Oh E, Choi G, Liang Z, Wang ZY. 2012. Interactions between HLH and bHLH factors modulate
456 light-regulated plant development. *Mol Plant*, 5, 688-697.
- 457 Holton TA, Brugliera F, Tanaka Y. 1993. Cloning and expression of flavonol synthase from *Petunia hybrida*.

- 458 *Plant J*, **4**, 1003–1010.
- 459 Hou S, Du W, Hao Y, Han Y, Li H, Liu L, Zhang K, Zhou M, Sun Z. 2021. Elucidation of the regulatory
460 network of flavonoid biosynthesis by profiling the metabolome and transcriptome in Tartary Buckwheat.
461 *J Agric Food Chem*, **69**, 7218-7229.
- 462 Huang Y, Wu Q, Wang S, Shi J, Dong Q, Yao P, Shi G, Xu S, Deng R, Li C, Chen H, Zhao H. 2019.
463 FtMYB8 from Tartary buckwheat inhibits both anthocyanin/proanthocyanidin accumulation and
464 marginal Trichome initiation. *BMC Plant Biol*, **19**, 263.
- 465 Jiang P, Burczynski F, Campbell C, Pierce G, Austria JA, Briggs CJ. 2007. Rutin and flavonoid contents in
466 three buckwheat species *Fagopyrum esculentum*, *F. tataricum*, and *F. homotropicum* and their protective
467 effects against lipid peroxidation. *Food Res Int*, **40**, 356-364.
- 468 Jin H, Cominelli E, Bailey P, Parr A, Mehrtens F, Jones J, Tonelli C, Weisshaar B, Martin C. 2000.
469 Transcriptional repression by AtMYB4 controls production of UV-protecting sunscreens in Arabidopsis.
470 *EMBO J*, **19**, 6150–6161.
- 471 Koes RE, Spelt CE, Mol JN. 1989. The chalcone synthase multigene family of *Petunia hybrida* (V30):
472 differential, light-regulated expression during flower development and UV light induction. *Plant Mol*
473 *Biol*, **12**, 213–225.
- 474 Kumar S, Stecher G, Tamura K. 2016. MEGA7: molecular evolutionary genetics analysis version 7.0 for
475 bigger datasets. *Mol Biol Evol*, **2016**, **33**, 1870-1874.
- 476 Liew CF, Loh CS, Goh CJ, Lim SH. 1998. The isolation, molecular characterization and expression of
477 dihydroflavonol 4-reductase cDNA in the orchid, *Bromheadia finlaysoniana*. *Plant Sci*, **135**, 161–169.
- 478 Li J, Luan Q, Han J, Zhang C, Liu M, Ren Z. 2020. CsMYB60 directly and indirectly activates structural
479 genes to promote the biosynthesis of flavonols and proanthocyanidins in cucumber. *Hortic Res*, **7**, 103.

- 480 Li P, Chen B, Zhang G, Chen L, Dong Q, Wen J, Mysore KS, Zhao J. 2016. Regulation of anthocyanin and
481 proanthocyanidin biosynthesis by *Medicago truncatula* bHLH transcription factor MtTT8. *New Phytol*,
482 210, 905-921.
- 483 Lotkowska ME, Tohge T, Fernie AR, Xue GP, Balazadeh S, Mueller-Roeber B. 2015. The Arabidopsis
484 transcription factor MYB112 promotes anthocyanin formation during salinity and under high light stress.
485 *Plant Physiol*, **169**, 1862–1880.
- 486 Ludwig SR, Habera LF, Dellaporta SL, Wessler SR. 1989. Lc, a member of the maize R gene family
487 responsible for tissue-specific anthocyanin production, encodes a protein similar to transcriptional
488 activators and contains the myc-homology region. *Proc Natl Acad Sci USA*, **86**, 7092–7096.
- 489 Luo X, Zhao H, Yao P, Li Q, Huang Y, Li C, Chen H, Wu Q. 2018. An 2R3-MYB transcription factor
490 FtMYB15 involved in the synthesis of anthocyanin and proanthocyanidins from Tartary buckwheat. *J*
491 *Plant Growth Regul*, **37**, 76–84.
- 492 Mona CM, Christopher JL. 1987. Chalcone isomerase cDNA cloning and mRNA induction by fungal
493 elicitor, wounding and infection. *EMBO J*, **6**, 1527–1533.
- 494 Montefiori M, Brendolise C, Dare AP, Lin-Wang K, Davies KM, Hellens RP, Allan AC. 2015. In the
495 Solanaceae, a hierarchy of bHLHs confer distinct target specificity to the anthocyanin regulatory
496 complex. *J Exp Bot*, **66**, 1427-1436.
- 497 Mortazavi A, Williams BA, McCue K, Schaeffer L, Wold B. 2008. Mapping and quantifying mammalian
498 transcriptomes by RNA-Seq. *Nat Methods*, **5**, 621-8.
- 499 Negahdari R, Bohlouli S, Sharifi S, Maleki Dizaj S, Rahbar Saadat Y, Khezri K, Jafari S, Ahmadian E,
500 Gorbani Jahandizi N, Raesi S. 2021. Therapeutic benefits of rutin and its nanoformulations. *Phytother*
501 *Res*, **35**, 1719-1738.

- 502 Nesi N, Debeaujon I, Jond C, Pelletier G, Caboche M, Lepiniec L. 2000. The TT8 gene encodes a basic
503 helix-loop-helix domain protein required for expression of DFR and BAN genes in Arabidopsis siliques.
504 *Plant Cell*, 12, 1863-1878.
- 505 Payne CT, Zhang F, Lloyd AM. 2000. GL3 encodes a bHLH protein that regulates trichome development in
506 Arabidopsis through interaction with GL1 and TTG1. *Genetics*, 156, 1349-1362.
- 507 Russell DW. 1971. The metabolism of aromatic compounds in higher plants. *J Biol Chem*, **246**, 3870–3878.
- 508 Shang Y, Venail J, Mackay S, Bailey PC, Schwinn KE, Jameson PE, Martin CR, Davies KM. 2011. The
509 molecular basis for venation patterning of pigmentation and its effect on pollinator attraction in flowers
510 of *Antirrhinum*. *New Phytol*, 189, 602-615.
- 511 Spelt C, Quattrocchio F, Mol JNM, Koes R. 2000. anthocyanin1 of petunia encodes a basic helix-loop-helix
512 protein that directly activates transcription of structural anthocyanin genes. *Plant Cell*, 12, 1619-1632.
- 513 Teng S, Keurentjes J, Bentsink L, Koornneef M, Smeekens S. 2005. Sucrose-specific induction of
514 anthocyanin biosynthesis in Arabidopsis requires the MYB75/PAP1 gene. *Plant Physiol*, **139**,
515 1840–1852.
- 516 Toledo-Ortiz G, Huq E, Quail PH. 2003. The Arabidopsis basic/helix-loop-helix transcription factor family.
517 *Plant Cell*, 15, 1749-1770.
- 518 Vimolmangkang S, Han Y, Wei G, Korban SS. 2013. An apple MYB transcription factor, MdMYB3, is
519 involved in regulation of anthocyanin biosynthesis and flower development. *BMC Plant Biol*, **13**, 176.
- 520 Yang CQ, Fang X, Wu XM, Mao YB, Wang LJ, Chen XY. 2012. Transcriptional regulation of plant
521 secondary metabolism. *J Integr Plant Biol*, **54**, 703–712.
- 522 Yang W, Su Y, Dong G, Qian G, Shi Y, Mi Y, Zhang Y, Xue J, Du W, Shi T, Chen S, Zhang Y, Chen Q, Sun
523 W. 2020. Liquid chromatography-mass spectrometry-based metabolomics analysis of flavonoids and

- 524 anthraquinones in *Fagopyrum tataricum* L. Gaertn. (Tartary buckwheat) seeds to trace morphological
525 variations. *Food Chem*, 331, 127354.
- 526 Yin Q, Han X, Han Z, Chen Q, Shi Y, Gao H, Zhang T, Dong G, Xiong C, Song C, Sun W, Chen S. 2020.
527 Genome-wide analyses reveals a glucosyltransferase involved in rutin and emodin glucoside biosynthesis
528 in Tartary buckwheat. *Food Chem*, **318**, 126478.
- 529 Wang L, Deng R, Bai Y, Wu H, Li C, Wu Q, Zhao H. 2022. Tartary Buckwheat R2R3-MYB gene FtMYB3
530 negatively regulates anthocyanin and proanthocyanin biosynthesis. *Int. J Mol Sci*. 23, 2775.
- 531 Wang N, Xu H, Jiang S, Zhang Z, Lu N, Qiu H, Qu C, Wang Y, Wu S, Chen X. 2017. MYB12 and MYB22
532 play essential roles in proanthocyanidin and flavonol synthesis in red - fleshed apple (*Malus sieversii* f.
533 *niedzwetzkyana*). *Plant J*, 90, 276-292.
- 534 Williams CA, Grayer RJ. 2004. Anthocyanins and other flavonoids. *Nat Prod Rep*, 21, 539-573.
- 535 Zhang D, Jiang C, Huang C, Wen D, Lu J, Chen S, Zhang T, Shi Y, Xue J, Ma W, Xiang L, Sun W, Chen S.
536 2019. The light-induced transcription factor FtMYB116 promotes accumulation of rutin in *Fagopyrum*
537 *tataricum*. *Plant Cell Environ*, 42, 1340-1351.
- 538 Zhang K, Logacheva MD, Meng Y, Hu J, Wan D, Li L, Janovská D, Wang Z, Georgiev MI, Yu Z, Yang F,
539 Yan M, Zhou M. 2018. Jasmonate-responsive MYB factors spatially repress rutin biosynthesis in
540 *Fagopyrum tataricum*. *J Exp Bot*, 69, 1955-1966.
- 541 Zhang LJ, Li XX, Ma B, Gao Q, Du HL, Han Y, Li Y, Cao Y, Qi M, Zhu Y, Lu H, Ma M, Liu L, Zhou J,
542 Nan C, Qin Y, Wang J, Cui L, Liu H, Liang C, Qiao Z. 2017. The Tartary buckwheat genome provides
543 insights into rutin biosynthesis and abiotic stress tolerance. *Mol Plant*, **10**, 1224-1237.
- 544 Zhou LL, Shi MZ, Xie DY. 2012. Regulation of anthocyanin biosynthesis by nitrogen in
545 TTG1-GL3/TT8-PAP1-programmed red cells of *Arabidopsis thaliana*. *Planta*, **236**, 825-837.

546 Zhou M, Sun Z, Wang C, Zhang X, Tang Y, Zhu X, Shao J, Wu Y. 2015. Changing a conserved amino acid
547 in R2R3-MYB transcription repressors results in cytoplasmic accumulation and abolishes their
548 repressive activity in Arabidopsis. *Plant J*, **84**, 395–403.

549 Zhou M, Zhang K, Sun Z, Yan M, Chen C, Zhang X, Tang Y, Wu Y. 2017. LNK1 and LNK2 corepressors
550 interact with the MYB3 transcription factor in phenylpropanoid biosynthesis. *Plant Physiol*, **174**,
551 1348–1358.

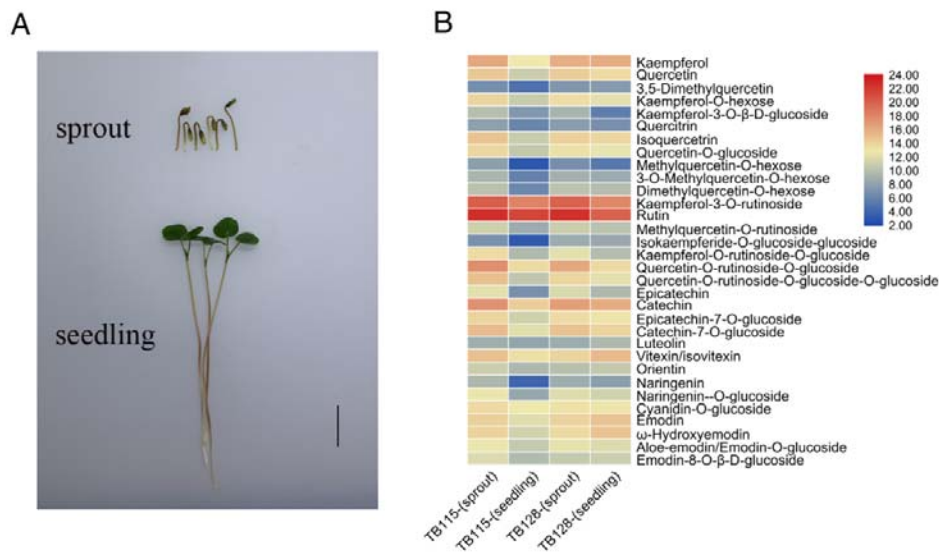
552 Zhou M, Memelink J. 2016. Jasmonate-responsive transcription factors regulating plant secondary
553 metabolism. *Biotechnol Adv*, **34**, 441–449.

554 Zhou M, Sun Z, Ding M, Logacheva MD, Kreft I, Wang D, Yan M, Shao J, Tang Y, Wu Y, Zhu X. 2017.
555 FtSAD2 and FtJAZ1 regulate activity of the FtMYB11 transcription repressor of the phenylpropanoid
556 pathway in *Fagopyrum tataricum*. *New Phytol*, 216, 814-828.

557 Zimmermann IM, Heim MA, Weisshaar B, Uhrig JF. 2004. Comprehensive identification of Arabidopsis
558 thaliana MYB transcription factors interacting with R/B-like BHLH proteins. *Plant J*, **40**, 22–34.

559

560



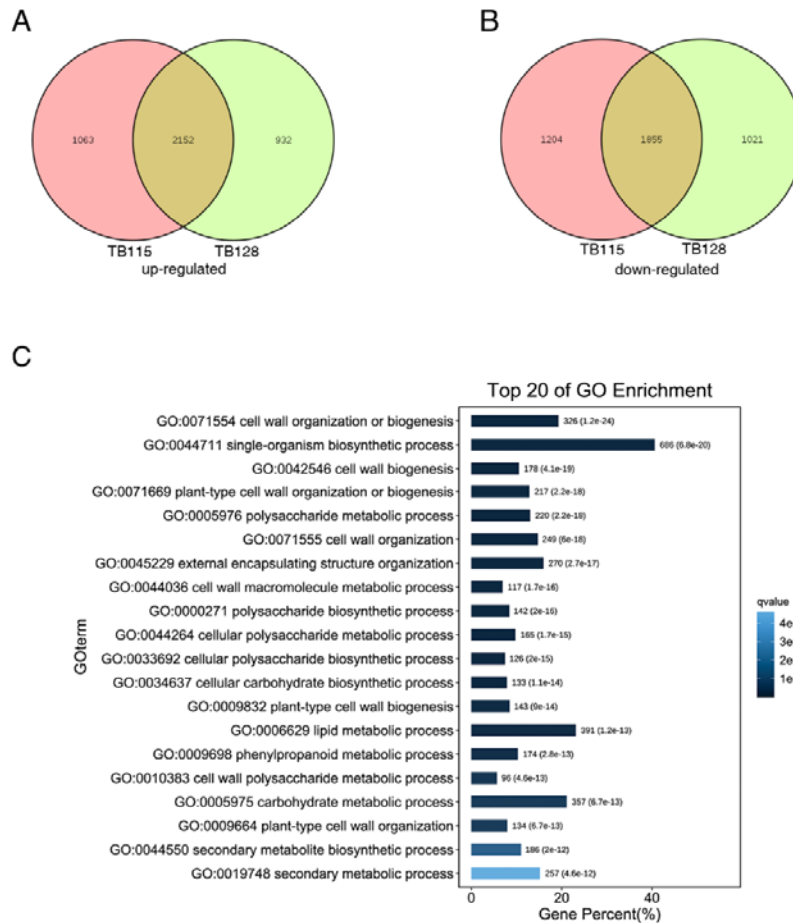
561

562 **Figure 1. Flavonoid content in Tartary buckwheat at the sprout and seedling stages.** (A) Photographs

563 of Tartary buckwheat at the sprouting and seedling stages. Scale bar = 2 cm. (B) Heat map of the content

564 of various flavonoids at the sprout and seedling stages of the TB115 and TB128 varieties. The depths of

565 color in the red and blue rectangles indicate higher and lower flavonoid content level.



566

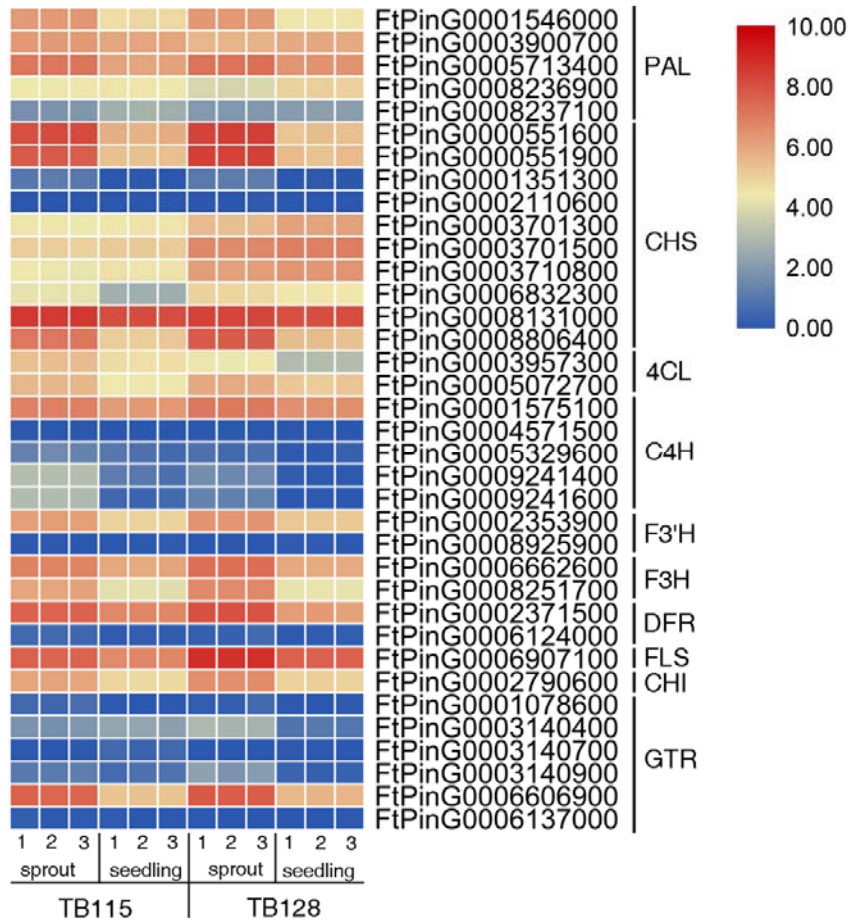
567 **Figure 2. Gene expression varied in sprouts from seedlings in two varieties TB115 and TB128, and**

568 **GO analysis among these differential genes. (A) Upregulated genes in the two varieties. Among these**

569 genes, 2,152 genes (brown) were upregulated in both varieties. (B) 3,059 and 2,876 genes were

570 downregulated genes in both varieties. 1,855 genes (brown) were overlapped. (C) GO analysis on the 2,152

571 upregulated genes. Top 20 of the GO enrichment were listed.



572

573 **Figure 3. Heat map of the expression levels of flavonoid synthesis genes at sprout and seedling stages.**

574

For each variety, the sprouting and seedling level were studied, the numbers (1-3) represent three biological

575

repeats. The depths of color in the red and blue rectangles indicate higher and lower z scores of RNA

576

expression level. PAL: phenylalanine ammonialyase; CHS: chalcone synthase; 4CL: 4-coumarate:CoA

577

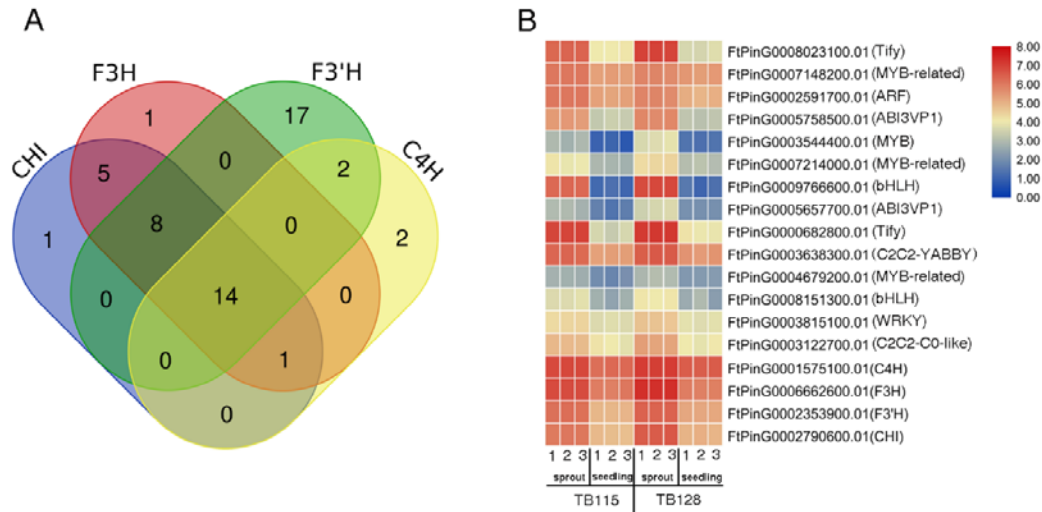
ligase; C4H: cinnamate-4-hydroxylase; F3' H: flavonoid-3'- hydroxylase; F3H: flavanone-3-hydroxylase;

578

DFR: dihydroflavonol reductase; FLS: flavonol synthase; CHI: chalcone isomerase; GTR: glucosyl

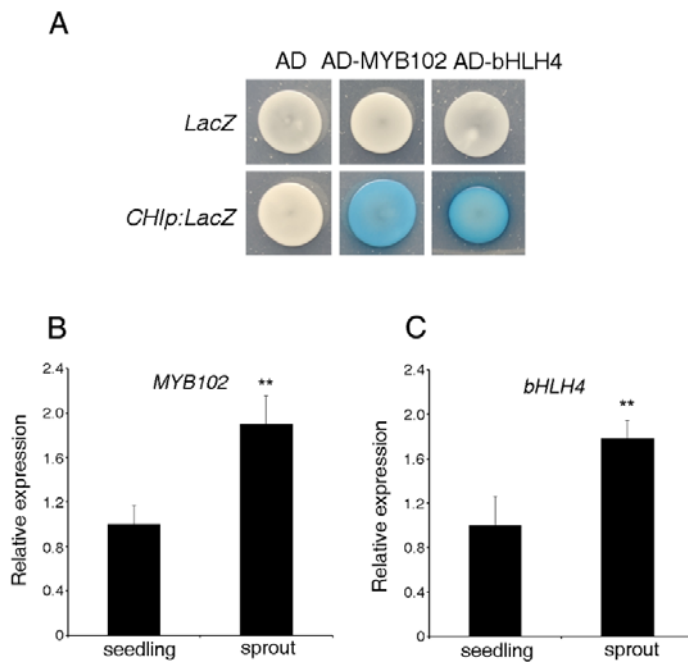
579

transferase



580

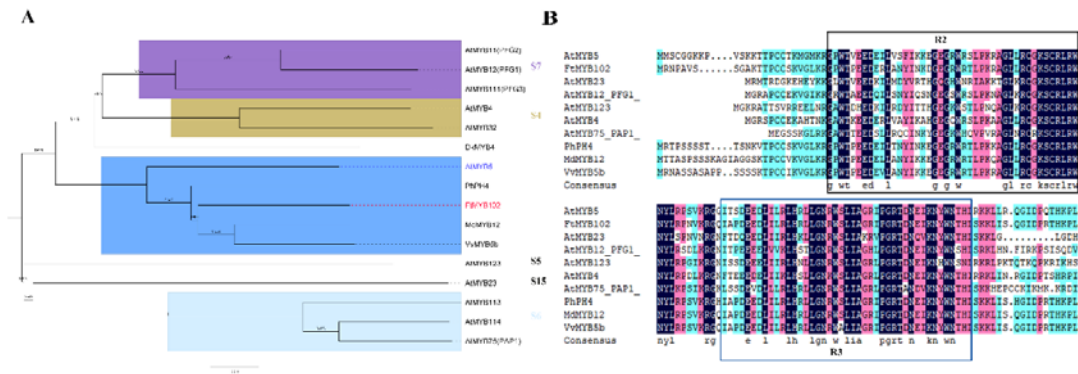
581 **Figure 4. Identification of transcription factors coexpressed with flavonoid synthase genes.** (A) The
 582 Venn diagram shows the number of genes coexpressed with CHI, F3H, F3'H, and C4H. (B) Heat map of
 583 the expression levels of the 14 TFs indicated between brackets, including CHI, F3H, F3'H, and C4H. The
 584 numbers one, two, and three represent three biological repeats. The depths of color in the red and blue
 585 rectangles indicate higher and lower z scores of RNA expression level.



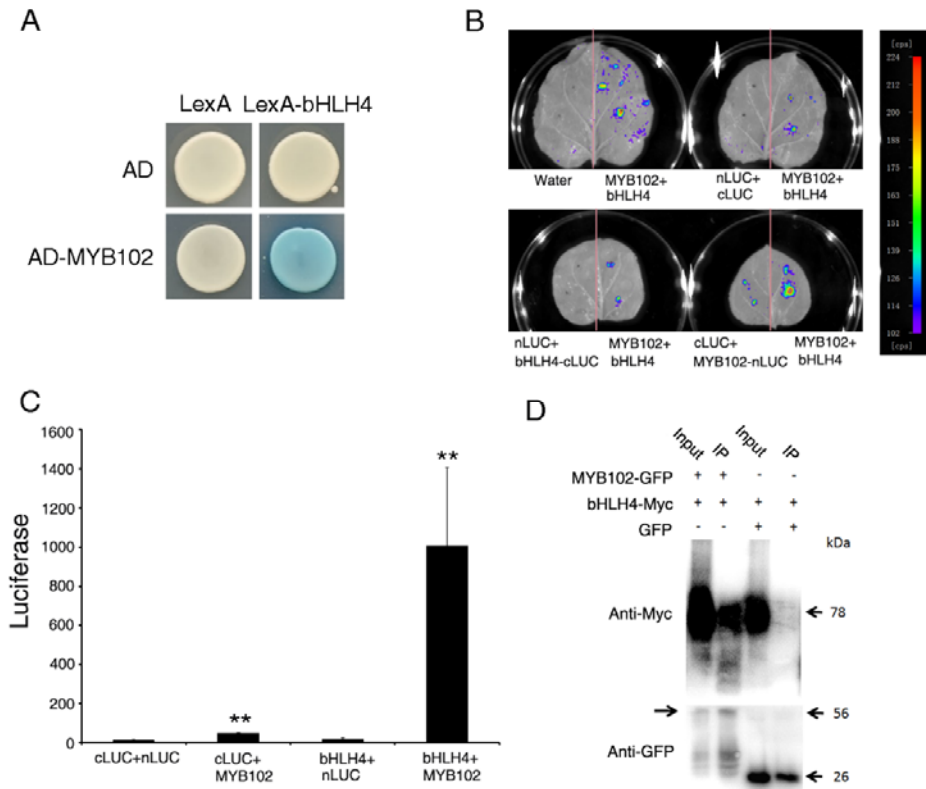
586

587 **Figure 5. FtMYB102 and FtbHLH4 are candidate transcription factors that regulate rutin synthesis.**

588 (A) Yeast one-hybrid assay showing that AD-MYB102 and AD-bHLH4 bind to the promoter regions of
 589 *CHI*. (B) and (C) MYB102 and *bHLH4* expression in sprout and seedling. The relative expression levels
 590 were normalized to those of the actin control. Data represent the means \pm standard deviation of biological
 591 triplicates.



592
 593 **Figure 6. Phylogenetic and structural domain analysis of FtMYB102.** (A) Phylogenetic analysis of
 594 FtMYB102 with MYB TFs in different subgroups and species. Three S7 group members: AtMYB11-12
 595 and AtMYB111 in *A. thaliana*; two S4 group members: AtMYB4 and At MYB32; one S5 and S15 group
 596 member AtMYB123 and AtMYB23, respectively; three S6 group members AtMYB75 and AtMYB113-114.
 597 FtMYB102, PhPH4(*Petunia hybrida*), MdMYB12(*Malus domestica*) and VvMYB5b(*Vitis vinifera*) were
 598 classified as AtMYB5. (B) The structural domain analysis of FtMYB102 showed it was a classic R2R3
 599 MYB TF.



600

601 **Figure 7. FtbHLH4 physically interacts with FtMYB102.** (A) Yeast two-hybrid assay using bHLH4 and

602 MYB102 constructs with AD: the B42 activation domain alone; AD-MYB102: MYB102 fused with the

603 B42 activation domain; LexA: the LexA DNA-binding domain alone; LexA-bHLH4: the LexA

604 DNA-binding domain fused to bHLH4. (B) Luciferase Complementation Imaging Assay (LCI assay) of

605 MYB102–nLUC with bHLH4–cLUC in tobacco leaves with Water, nLUC+ cLUC, nLUC+ bHLH4–cLUC

606 and cLUC+ MYB102–nLUC served as controls; MYB102–nLUC + bHLH4–cLUC in the four leaves were

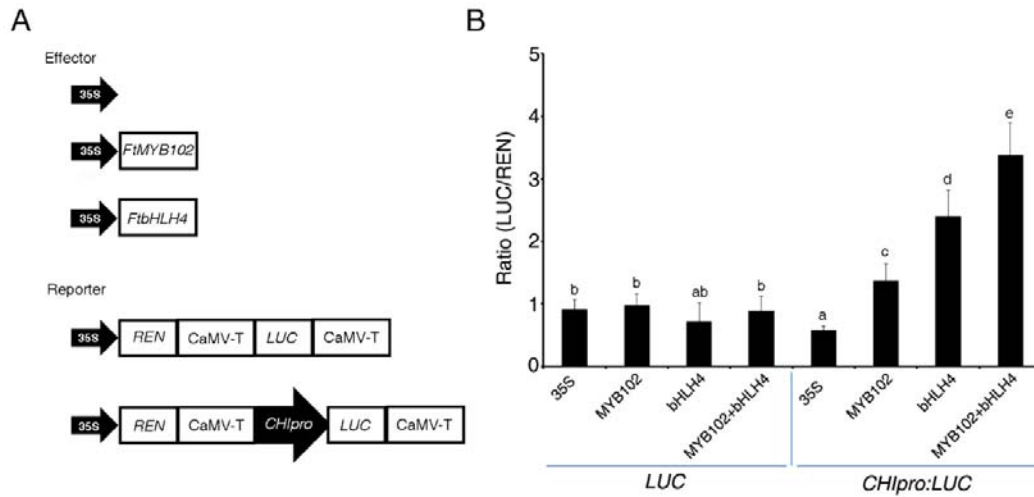
607 four biological repeats. (C) The interaction between MYB102 and bHLH4 was quantitatively detected

608 using LCI. Data represent the means \pm standard deviation of biological triplicates. (D) Co-IP assay with

609 MYB102-GFP and bHLH4-Myc coexpression in tobacco leaves. +: the corresponding component was

610 added to the reaction system; -: no corresponding component added; the number on the right represents the

611 size of the proteins.



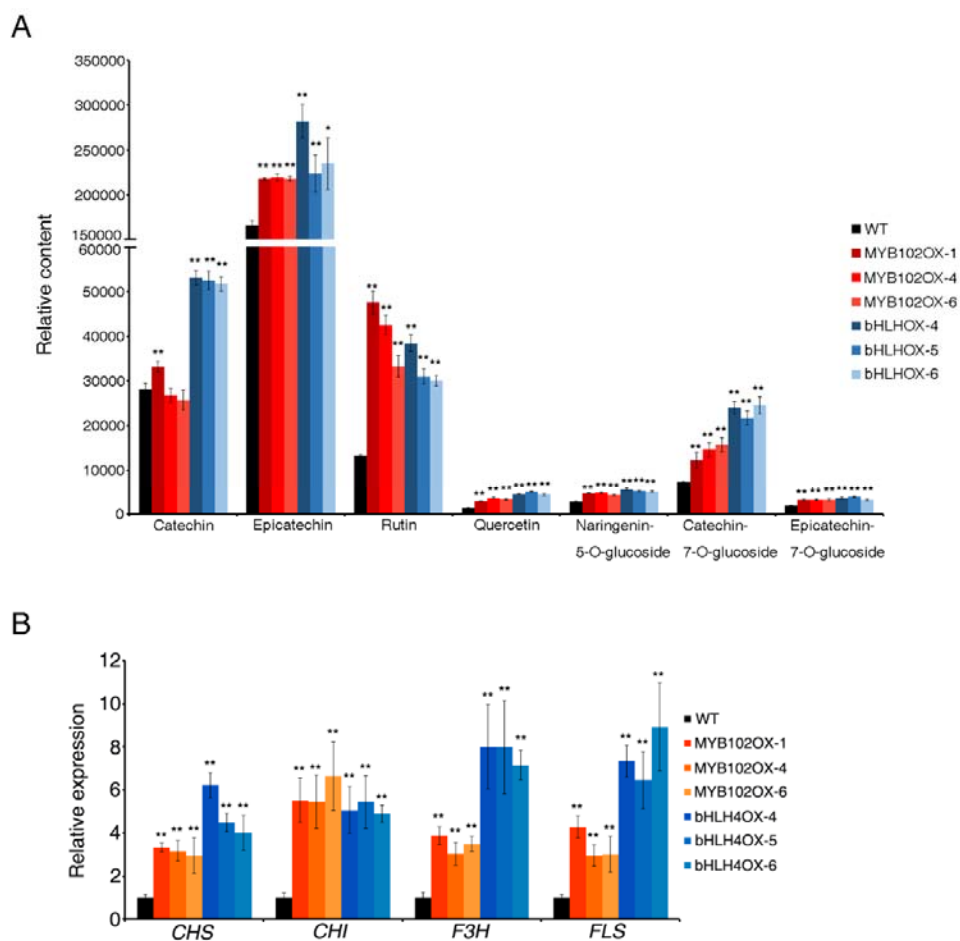
612

613 **Figure 8. MYB102 and bHLH4 coordinately activate the expression of *CHI*.** (A) Schematic diagrams

614 of the effector and reporter plasmids used in dual-LUC assays. REN, Renilla luciferase; LUC, firefly

615 luciferase. (B) Dual-LUC assay in tobacco leaves using the constructs shown in (A). The 35S effector was

616 used as a negative control. Data represent the means \pm standard deviation of biological triplicates.



617

618 **Figure 9. Overexpression of MYB102 and bHLH4 can promote flavonoid biosynthesis in Tartary**

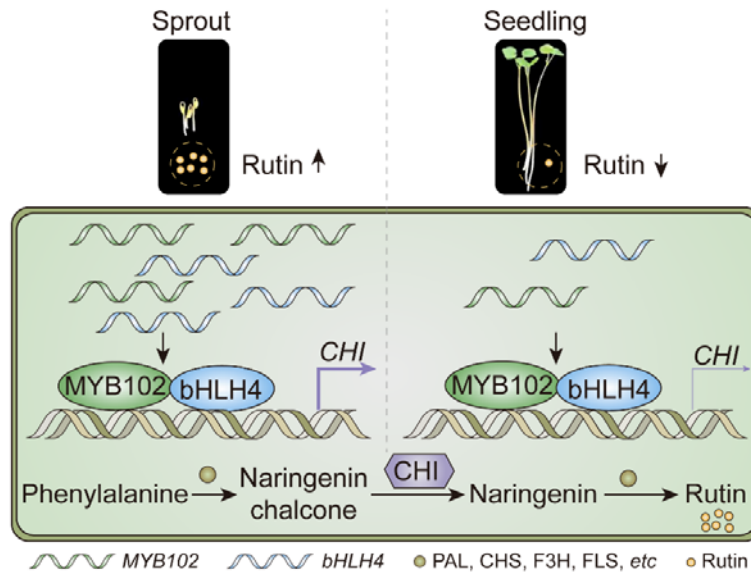
619 **buckwheat hairy roots. (A) Relative flavonoid content in MYB102 and bHLH4 overexpression lines in**

620 **Tartary buckwheat hairy roots. Double asterisks indicate a significant difference at $P < 0.01$ using the**

621 **Student's t test-test. (B) Detection of gene expression related to flavonoid synthesis pathways in MYB102**

622 **and bHLH4 transgenic lines. The relative expression levels were normalized to that of the actin control.**

623 **Data represent the means \pm standard deviation of biological triplicates.**



624

625 **Figure 10. A working model of the MYB102 and bHLH4 form a transcriptional complex by inducing**

626 **CHI expression to promote the accumulation of rutin.** (Left) In sprouts, the transcripts of MYB102 and

627 bHLH4 are abundant, thus more MYB102 and bHLH4 proteins form a complex to activate the high

628 expression of *CHI*, since *CHI* is an important structural gene for rutin, this causes rutin levels to be high.

629 (Right) In seedlings, unlike sprouts, MYB102 and bHLH4 transcripts are reduced, and *CHI* expression is

630 downregulated as the number of MYB102 and bHLH4 complexes is less; thus, rutin levels are reduced.

631

632